d Collection

An Extremely Miniaturized Microstrip

Balun Filter

by Xin Guan

Under the Supervision of Prof. In-Ho Kang

Department of Radio Sciences and Engineering

in Graduate School of

Korea Maritime University

June 2012

Contents

Nomenclature

Z_0 :   Characteristic impedance

Z_{oe} :   Even-mode characteristic impedance

Z_{oo} :   Odd-mode characteristic impedance

Y_0 :   Characteristic admittance

Y_{oe} :   Even-mode characteristic admittance

Y_{oo} :   Odd-mode characteristic admittance

θ :   Electrical length

ω :   Angular frequency

C :   Capacitance

L :   Inductance

S :   Scattering parameter

K :   Coupling coefficient

List of Tables

List of Figures

Abstract

The field of RF (radio frequency) and microwave is rapidly growing because of its use in wireless communication systems. In wireless applications, baluns which frequently connect a bandpass filter with a balanced component are significant system factors but usually occupy much of the volume of the systems. Thus, with the speedy development of modern communication, reducing the size of balun is the main challenge in making RF systems compact. In addition, the poor balanced port matching and isolation performance of many conventional baluns limits their application.

In this thesis, a novel enhanced balun bandpass filter for extremely miniaturization is demonstrated utilizing the combination of diagonally shorted coupled lines and parallel end shorted coupled lines both with shunt lumped capacitors. This method can largely reduce the required electrical length of transmission line, not only approximately maintaining the same characteristic around the center frequency but also effectively suppressing the spurious passband. Meanwhile, a resistive network between the outputs is presented to realize the balanced matching and isolation. Comparing with the typical Marchand Balun, it takes better performance as well as shows a wider upper stopband.

Design equations and method is fully explained in this thesis. An extremely miniaturized balun filter operating at 1GHz of microstrip line form is fabricated on PCB substrate with 15 degree electrical length of the coupled lines. Both

theoretical and measured performances are displayed. The experimental verification proves the usefulness of the proposed balun filter and its advantages of the application for mobile communications, etc.

CHAPTER 1 Introduction

Baluns are key components in many wireless and mobile communication systems as well as microwave, millimeter-wave and RF circuits such as double balanced mixers [1][2], push-pull amplifiers [3], frequency doublers [4], multipliers and antenna excitations in order to reduce the noise and higher-order harmonics and improve the dynamic range of the systems. Functionally, a balun is a device intended to act as a transformer, matching an unbalanced circuit to a balanced one, or vice versa, with minimum loss and equal balanced impedances. The signal of a balanced circuit structure comprises two signal components with the same magnitude but 180 phase difference [5] [6].

It was desirable that the balun have a wide-band characteristic so as to make unnecessary any adjustments on the balun over a range of frequencies covered by adjusting the multifarious applications. Certain previously described wide-band transformers require a considerable amount of space because of the use of the frequency-compensating effects of one or two quarter-wave transmission line sections connected between the balun and the balanced load [7].

1.1 Background and Introduction of Balun

There are several types of baluns that are either active or passive. The major advantage of active baluns is the small size, which makes them suitable to integrate into ICs. However, the performances of active baluns including linearity, noise figure, and balance property are usually not satisfactory as well as exhaust more

energy [8]. Passive baluns can be classified as lumped-type [9], coil-type [10], and distributed-type baluns [6]. The advantages of a lumped-type balun are small volume and light weight. However, it is not easy to maintain 180 phase difference and identical magnitude between the two signals. Coil-type baluns have been widely used in lower frequency and ultra high frequency (UHF) bands. When a coil-type balun is used in higher than the UHF band, it usually has a drawback of having considerable loss. Distributed-type baluns can further be classified as a 180 hybrid balun and a Marchand balun. A 180 hybrid balun has a fairly good frequency response in the microwave frequency band. However, its size often poses a problem when it is used in the radio frequency range between 200 MHz and several GHz.

Among the various kinds of baluns, a planar version of Marchand balun, illustrated in Fig. 1.1, has been adopted for a long time due to its planar structure, good amplitude, phase balance characteristics and inherently wide operation bandwidth. Both phase difference and power distribution of a Marchand balun are reasonably good. A Marchand balun is commonly used in the industry comprises two sections of quarter-wave coupled lines [11] which may be realized using parallel-coupled microstrip lines [12], Lange couplers [13], multilayer coupled structures [14], or spiral coils [9]. Nevertheless, the Marchand balun consisting of two identical $\lambda/4$ coupled lines still occupies a big area, especially at low frequencies.
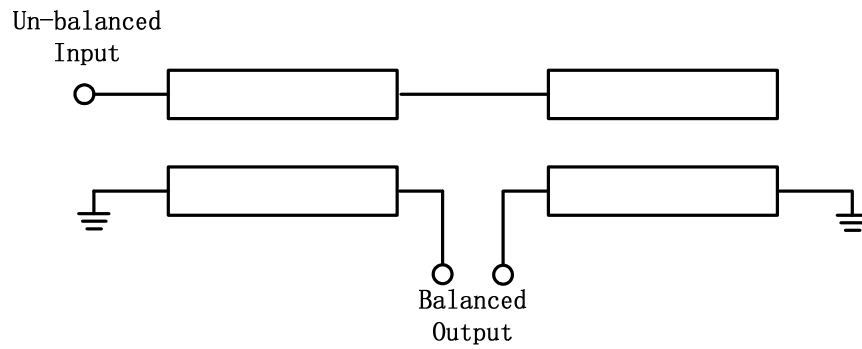
Fig. 1.1 A planar version of Marchand balun

The first transmission line balun was described in the literature by Lindenblad [15] in 1939 and variations on his original scheme soon followed. Among these was that of Marchand, who introduced a series open-circuited line to compensate for the short circuited line reactance of the two wires. Three other variations were cataloged and described by the Harvard Radio Research Laboratory staff [16]. Harvard's Type II balun is similar to Marchand's variation but without compensation. Because of the compensating feature of Marchand's variation, the author suggests the name "compensated balun" to distinguish it from the others. In 1957, Roberts [7] apparently reinvented the compensated balun and the author used Roberts' paper as a starting point of his initial analysis [17]. In 1958, McLaughlin, Dunn, and Grow [18], using Marchand's paper, designed a 13-to-l bandwidth compensated balun which is the broadest thus far published. Bawer and Wolfe [19] subsequently applied the compensated balun to a broadband spiral antenna.

In design of a coupled-line Marchand balun, various analysis methods were presented. They are usually designed through circuit simulations using full-wave

electromagnetic analysis [1] or lumped-element models [9]. Various synthesis techniques using coupled-line equivalent-circuit models and analytically derived scattering parameters have also been reported [20]. In [2], use of the relationships of the power wave in a balun to derive the scattering parameters can analyze a symmetrical Marchand balun, but the exact prediction is only valid at the center frequency. In [21], inclusion of the parameter of the electrical length of the transmission line can predict broadband performances, but the approach lacks generality. Furthermore, to achieve wider bandwidth, multiconductor coupled lines to realize tight couplings were presented. Another method is the even- and odd-mode analysis method. However, it is limited to the case of a symmetrical coupled-line Marchand balun with the maximally flat responses.

In addition, most of the work on improving the planar Marchand balun has focused on achieving wide-band performance and miniaturization. The issue of balun output matching and isolation has not been addressed. This may be attributed to the well-known fact that a lossless reciprocal three-port network such as the balun cannot achieve perfect matching at all three ports. In many applications, however, balun output matching and isolation can enhance circuit performance. In double-balanced diode mixers, good output matching of the local oscillator (LO) and RF baluns at the diode interfaces can reduce LO power drive requirements and improve conversion loss. In push–pull amplifiers, isolation between the transistors provided by the balun outputs can enhance amplifier stability. In [22], a resistive network connected between the balun outputs is proposed to achieve balun output

4

matching and isolation. Combining this technique with impedance transforming Marchand baluns, a class of perfectly matched impedance-transforming baluns can be realized. Whereas, this bulky resistive network consumes a large circuit area.

In some wireless applications, especially for WLAN and Bluetooth systems, the balun frequently connects a bandpass filter (BPF) with a balanced component, such as low noise amplifier (LNA), monolithic microwave integrated circuit (MMIC). Hence an integration of a BPF and a balun is necessary to reduce the cost and the size of the functional block in the systems. Recently, to meet the need, a balanced filter has been reported. However, the balanced filter, simply, uses an integration concept of the two components using an inter-matching circuit and, hence, the resultant filter is a very complicated component.

In this thesis, a novel balun filter for size extremely miniaturization is demonstrated utilizing the combination of diagonally shorted coupled lines and parallel end shorted coupled lines. The method of adding lumped capacitors to the conventional coupled line section can largely reduce the required electrical length of coupled line while maintaining approximately the same characteristic around the center frequency and effectively suppress the spurious passband. Furthermore, by employing an improved resistive isolation network between the two balanced ports, the perfect balanced ports matching and isolation can be achieved. Theoretical analysis and design formulas are derived. To prove the feasibility and validity of the design equation, experimental verification of such a compact balun filter working at 1GHz is presented. It is simulated by ADS and HFSS and implemented

5

on printed circuit board (PCB). The fabricated balun filer has a small area of 10mm×30mm, not including the extended space for testing, a wider upper stopband and phase difference of 180 degree at the two balanced ports over the operating frequency band. The measurement results agree well with the simulation, which demonstrates that the proposed filter has great application potential.

1.2 Organization of the Thesis

The contents of the thesis are illustrated as follows:

Chapter 1 briefly introduces the background, motivation and outline of this work.

Chapter 2 describes the size-reduction method for quarter-wave transmission line by using diagonally shorted coupled lines and parallel end shorted coupled lines both with shunt lumped capacitors. Then it presents the design procedure of such a new configuration balun filter. This chapter also introduces an improved resistive network for balanced ports matching and isolation.

Chapter 3 displays the simulated results by ADS and HFSS and the experimental and measured results of fabricated balun filter.

Chapter 4 gives the conclusion of this work.

CHAPTER 2 Balun Filter Design Theory

The conventional parallel coupled lines are useful and widely applied structures that provide the basis for many types of components, including directional couplers, power splitters and combiners, duplexers, filters, phase shifters, transformers and the aforementioned baluns. The microstrip parallel coupled filter is first proposed by Cohn in 1958 [23]. This type of filter is popular because of its planar structure, insensitivity to fabrication tolerance, wide realizable bandwidth [24]–[26], and simple synthesis procedures [27]. However, despite its advantages, the traditional parallel coupled-line filter has several shortcomings. One of the disadvantages is that it suffers from spurious responses that are generated at the multiples of operating frequency due to the unequal even- and odd-mode phase velocities of the coupled line. The stopband rejection performance is thus severely degraded. Another is the whole length of the filter is too long. Both disadvantages greatly limit the application of this type of filter. To overcome these problems, the size reduction methods are introduced in this chapter.

2.1 Size Reduction Method

The quarter-wavelength transmission line has been playing a very important role in many microwave circuits, functioning as impedance transformers, phase inverters and so on. However, in many cases, it is too large to be compatible with other parts of microwave systems. The size reduction method proposing by Hirota [28] is attractive in view of using short transmission line and lumped capacitors.

7

But the circuit size could not be much reduced due to the limitation of the high impedance of the transmission line.

2.1.1 Diagonally Shorted Coupled Lines with Lumped Capacitors

The reduced quarter-wavelength transmission line using combination of shorted transmission line and shunt lumped capacitors proposed by Hirota is shown in Fig. 2.1. The related equations are as follows,

$$Z_A = \frac{Z_0}{\sin \theta_A} \tag{2.1}$$

$$\omega C_{A1} = \frac{\cos \theta_A}{Z_0} \tag{2.2}$$

where Z_A, Z_0, θ_A and ω are the characteristic impedance of the shorted transmission line, the characteristic impedance of the quarter-wavelength line, the electrical length of the shorted line and angular frequency, respectively.

(a)

(b)
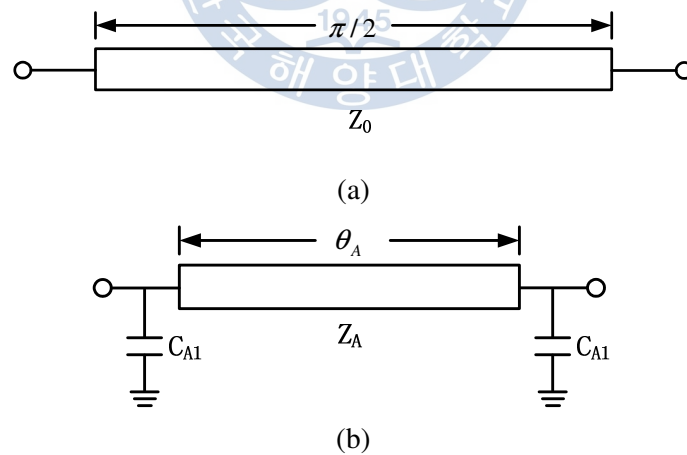
Fig. 2.1 Quarter-wave transmission line (a) and its equivalent shorted transmission line circuit (b)

8

From (2.1), it is clear that the characteristic impedance of the shorted transmission line Z_A goes higher as the electrical length θ goes smaller. When it is highly miniaturized, the impedance Z_A will too high to obtain. In order to reach very small electrical length up to several degrees, the coupled line component was adopted.

Fig. 2.2 (a) and (b) show the diagonally shorted coupled lines and its equivalent circuit [29].

(a)

(b)
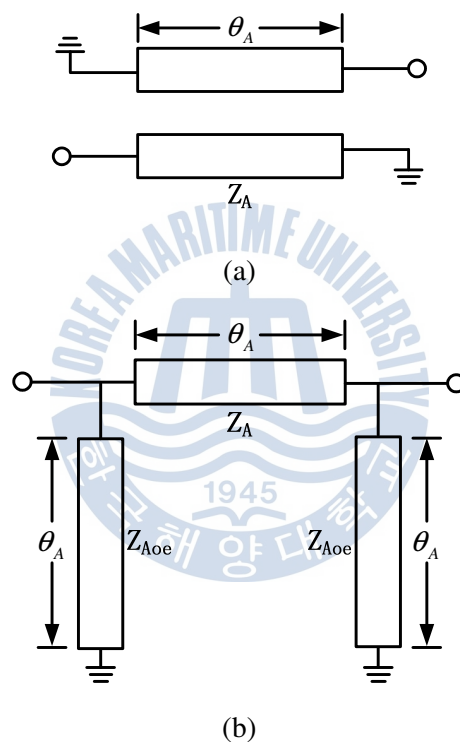
Fig. 2.2 Diagonally shorted coupled lines (a) and its equivalent circuit (b)

The characteristic impedance of the diagonally shorted coupled lines can be represented by the even-mode and odd-mode characteristic impedance and thus is given by:

9

$$Z_A = \frac{2Z_{Aoe}Z_{Aoo}}{Z_{Aoe} - Z_{Aoo}} \tag{2.3}$$

In Fig. 2.3, the artificial resonance circuits are inserted to Hirota's lumped distributed transmission line. Compare the dotted box part in Fig. 2.3 and the equivalent circuit of the coupled lines in Fig. 2.2 (b). If the following equation is satisfied, the dotted box part in Fig. 2.3 can be replaced by the coupled lines [30].

$$\omega C_{A0} = \frac{1}{\omega L_{A0}} = \frac{1}{Z_{Aoe} \tan \theta_A} \tag{2.4}$$

Fig. 2.3 Equivalent circuit of Hirota's reduced-size transmission line including artificial resonance circuits

Fig. 2.4 Final diagonally shorted miniaturized coupled lines with lumped capacitors equivalent to quarter-wave transmission line

10

Finally, the two capacitors in each side of the Fig. 2.3 can combine mathematically. The structure of the diagonally miniaturized coupled lines with lumped capacitors appears as shown in Fig 2.4.

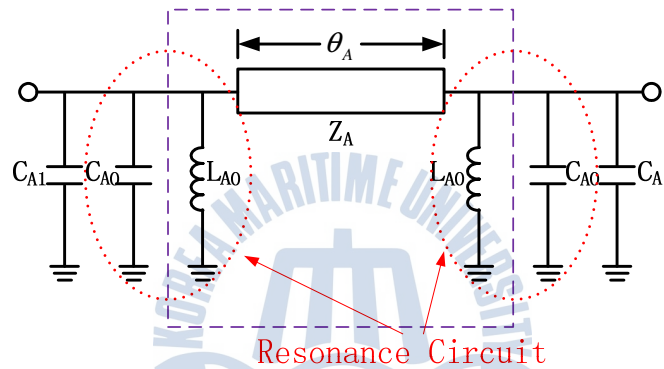$$C_A = C_{A0} + C_{A1} = \frac{1}{\omega Z_{Aoe} \tan \theta_A} + \frac{\cos \theta_A}{\omega Z_0} \tag{2.5}$$

2.1.2 Parallel End Shorted Coupled Lines with Lumped Capacitors

As is well known, the quarter-wavelength transmission line also can be made equivalent to a lumped circuit, as given in Fig. 2.5, and the value of C_{B1} is given by

$$\omega C_{B1} = \frac{1}{Z_0} \tag{2.6}$$
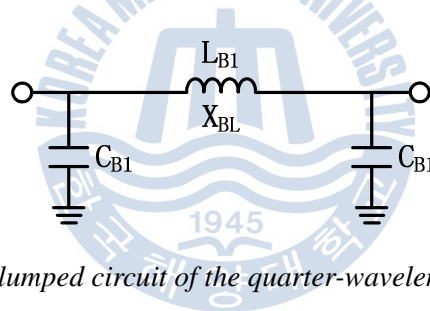
Fig. 2.5 Equivalent lumped circuit of the quarter-wavelength transmission line

In order to replace the lumped inductor, firstly, the artificial resonance circuits are inserted to the circuit again at each side of the lumped inductor, as illustrated in Fig. 2.6. Furthermore, the dotted network can be made equivalent to the parallel end shorted coupled line section with electrical length of θ_B in Fig. 2.7 (a) and (b) when (2.7) and (2.8) are satisfied [31].

$$X_{B0} = Z_{Boe} \tan \theta_B \qquad (2.7)$$

$$X_{BL} = \frac{2Z_{Boe}Z_{Boo}}{Z_{Boe} - Z_{Boo}} \tan \theta_B \qquad (2.8)$$

where Z_{Boe}, Z_{Boo} are even- and odd-mode impedances of the parallel end shorted coupled line, respectively.
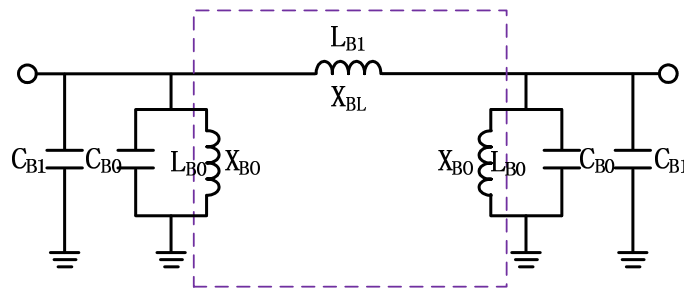
Fig. 2.6 Equivalent circuit of a quarter-wavelength transmission line with artificial resonance circuits inserted
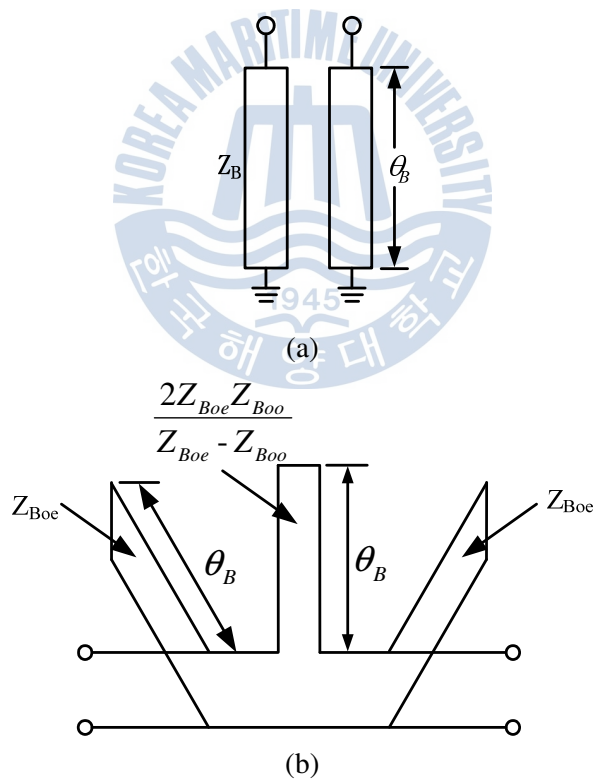
Fig. 2.7 Parallel end shorted coupled lines (a) and its equivalent circuit (b)

Fig. 2.8 is the schematic diagram of the initial miniaturized bandpass filter configuration and the value of the capacitors can be deduced from (2.7) as:

$$\omega C_{B0} = \frac{1}{Z_{Boe} \tan \theta_B} \tag{2.9}$$

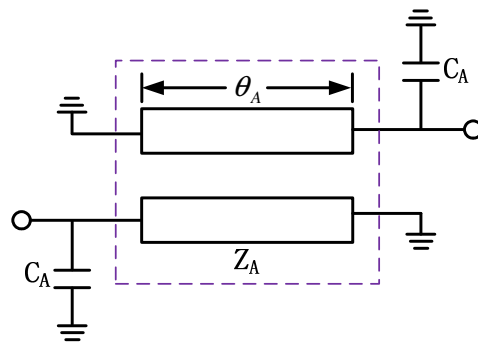$$C_B = C_{B0} + C_{B1} = \frac{1}{\omega Z_{Boe} \tan \theta_B} + \frac{1}{\omega Z_0} \tag{2.10}$$
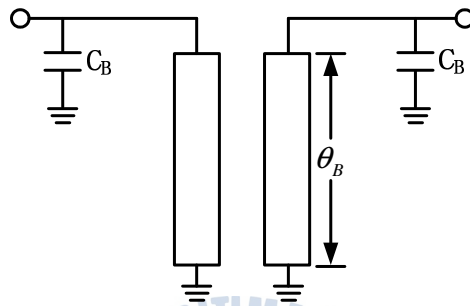
Fig. 2.8 Final parallel end shorted miniaturized coupled lines with lumped capacitors equivalent to quarter-wave transmission line

With (2.8), if defining the relationship between the characteristic impedance of the coupled-line and its even- and odd-mode impedances, we get:

$$Z_B = \frac{2Z_{Boe}Z_{Boo}}{Z_{Boe} - Z_{Boo}} = \frac{Z_0}{\tan \theta_B} \tag{2.11}$$

When the electrical length θ_B is very small for compact size, Z_B becomes very large. This large Z_B can be easily achieved by making Z_{Boe} and Z_{Boo} nearly the same.

13

2.2 Ordinary Balun Design

Among the various kinds of baluns, a planar version of Marchand balun has been adopted for a long time due to its various advantages. This kind of balun has been well developed in [22]. A block diagram of the balun is shown in Fig. 2.9. It provides balanced outputs to load terminations Z_2 from an unbalanced input with source impedance Z_1. In general, the impedances Z_1 and Z_2 are different. Thus, in addition to providing balanced outputs, the balun also needs to perform impedance transformation between the source and load impedances.
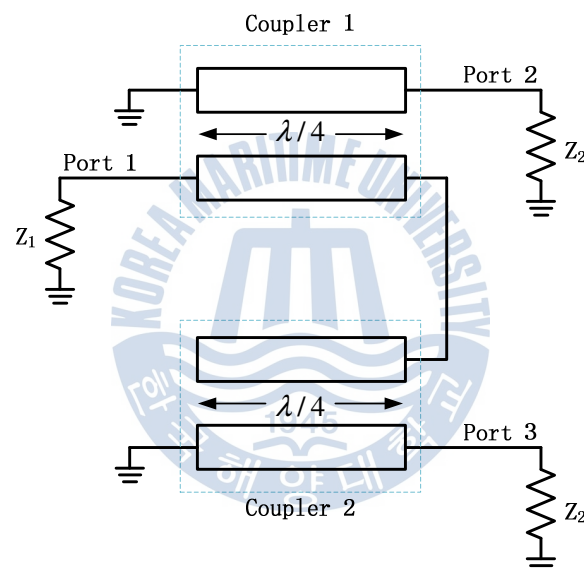
Fig. 2.9 Block diagram of a symmetrical Marchand balun as two identical couplers

As shown in Fig. 2.9, the planar Marchand balun consists of two coupled sections, each of which is one quarter-wavelength long at the center frequency of operation. For symmetrical baluns, the scattering matrix of the balun can be derived from the scattering matrix of two identical couplers. We just consider the case

where the source and load impedances are equal to Z_1. The scattering matrix for ideal couplers with infinite directivity and coupling factor k is given by

$$[S]_{coupler} = \begin{bmatrix} 0 & k & -j\sqrt{1-k^2} & 0 \\ k & 0 & 0 & -j\sqrt{1-k^2} \\ -j\sqrt{1-k^2} & 0 & 0 & k \\ 0 & -j\sqrt{1-k^2} & k & 0 \end{bmatrix} \quad (2.12)$$

The S-parameters of the balun can then be obtained, which has the form

$$[S]_{balun} = \begin{bmatrix} \dfrac{1-3k^2}{1+k^2} & j\dfrac{2k\sqrt{1-k^2}}{1+k^2} & -j\dfrac{2k\sqrt{1-k^2}}{1+k^2} \\ j\dfrac{2k\sqrt{1-k^2}}{1+k^2} & \dfrac{1-k^2}{1+k^2} & \dfrac{2k^2}{1+k^2} \\ -j\dfrac{2k\sqrt{1-k^2}}{1+k^2} & \dfrac{2k^2}{1+k^2} & \dfrac{1-k^2}{1+k^2} \end{bmatrix} \quad (2.13)$$

Equation (2.13) shows that the use of identical coupled sections results in balun outputs of equal amplitude and opposite phase, regardless of the coupling factor and port terminations. To achieve optimum power transfer of -3 dB to each port, we require

$$\left| S_{balun,21} \right| = \left| S_{balun,31} \right| = \frac{1}{\sqrt{2}} \quad (2.14)$$

With (2.13) and (2.14), the required coupling factor for optimum balun performance is given by

$$k = \frac{1}{\sqrt{3}} \quad (2.15)$$

When (2.15) is satisfied, the balun S matrix with parameters given by (2.13) reduces to

15

$$[S]_{balun} = \begin{bmatrix} 0 & \dfrac{j}{\sqrt{2}} & \dfrac{-j}{\sqrt{2}} \\[2ex] \dfrac{j}{\sqrt{2}} & \dfrac{1}{2} & \dfrac{1}{2} \\[2ex] \dfrac{-j}{\sqrt{2}} & \dfrac{1}{2} & \dfrac{1}{2} \end{bmatrix} \qquad (2.16)$$

2.3 New Structure for Miniaturized Balun Filter

As the two kinds of miniaturized coupled lines mentioned in the previous section of this chapter are input-output ports symmetrical structures, we will combine the two kinds of coupled lines by one of their alternative ports as the imbalanced input, and regard the other port of each coupled lines as the balanced outputs. A tri-port circuit is obtained acting as the new miniaturized balun filter, as depicted its outline in Fig. 2.10. Then the theoretical analysis and formula demonstration are described as follow to prove it has the function of balun.
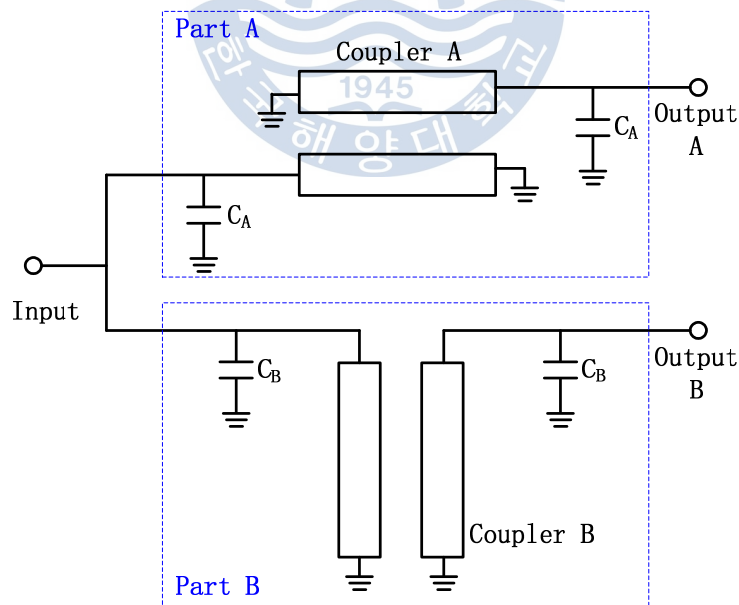

Fig. 2.10 New structure for miniaturized balun filter

16

The corresponding Y parameters of two kinds of coupled lines expressed in terms of the even- and odd-mode characteristic admittances Y_{oe} and Y_{oo} are given as in [32]

$$[Y_{couplerA}] = \begin{bmatrix} Y_{A11} & Y_{A12} \\ Y_{A21} & Y_{A22} \end{bmatrix} = \begin{bmatrix} -j\dfrac{Y_{Aoo}+Y_{Aoe}}{2}\cot\theta_A & -j\dfrac{Y_{Aoo}-Y_{Aoe}}{2}\csc\theta_A \\ -j\dfrac{Y_{Aoo}-Y_{Aoe}}{2}\csc\theta_A & -j\dfrac{Y_{Aoo}+Y_{Aoe}}{2}\cot\theta_A \end{bmatrix} \quad (2.17)$$

$$[Y_{couplerB}] = \begin{bmatrix} Y_{B11} & Y_{B12} \\ Y_{B21} & Y_{B22} \end{bmatrix} = \begin{bmatrix} -j\dfrac{Y_{Boo}+Y_{Boe}}{2}\cot\theta_B & j\dfrac{Y_{Boo}-Y_{Boe}}{2}\cot\theta_B \\ j\dfrac{Y_{Boo}-Y_{Boe}}{2}\cot\theta_B & -j\dfrac{Y_{Boo}+Y_{Boe}}{2}\cot\theta_B \end{bmatrix} \quad (2.18)$$

After shunting the capacitors at each side of the coupled lines, the Y parameters of two parts are

$$[Y_A] = \begin{bmatrix} Y_{A11}+j\omega C_A & Y_{A12} \\ Y_{A21} & Y_{A22}+j\omega C_A \end{bmatrix} \quad (2.19)$$

$$[Y_B] = \begin{bmatrix} Y_{B11}+j\omega C_B & Y_{B12} \\ Y_{B21} & Y_{B22}+j\omega C_B \end{bmatrix} \quad (2.20)$$

As a series of relationship about the properties of two kinds of coupled lines are deduced above, every element of Y parameters in (2.19) and (2.20) can be worked out

$$Y_{A11}+j\omega C_A = Y_{A22}+j\omega C_A = -j\frac{Y_{Aoo}+Y_{Aoe}}{2}\cot\theta_A + j\left(\frac{1}{Z_{Aoe}\tan\theta_A}+\frac{\cos\theta_A}{Z_0}\right)$$

$$= j\left(-\frac{1}{2}Y_{Aoo}\cot\theta_A - \frac{1}{2}Y_{Aoe}\cot\theta_A + Y_{Aoe}\cot\theta_A + \frac{\cos\theta_A}{Z_0}\right) \quad (2.21)$$

$$= j\left(-\frac{Y_{Aoo}-Y_{Aoe}}{2}\frac{\cos\theta_A}{\sin\theta_A}+\frac{\cos\theta_A}{Z_0}\right) = j\left(-\frac{\cos\theta_A}{Z_A\sin\theta_A}+\frac{\cos\theta_A}{Z_0}\right) = 0$$

$$Y_{A12} = Y_{A21} = -j\frac{Y_{Aoo}-Y_{Aoe}}{2}\csc\theta_A = -j\frac{Y_A}{\sin\theta_A} = -jY_0 \quad (2.22)$$

17

$$Y_{B11} + j\omega C_B = Y_{B22} + j\omega C_B = -j\frac{Y_{Boo} + Y_{Boe}}{2}\cot\theta_B + j(\frac{1}{Z_{Boe}\tan\theta_B} + \frac{1}{Z_0})$$

$$= j(-\frac{1}{2}Y_{Boo}\cot\theta_B - \frac{1}{2}Y_{Boe}\cot\theta_B + Y_{Boe}\cot\theta_B + \frac{1}{Z_0}) \qquad (2.23)$$

$$= j(-\frac{Y_{Boo} - Y_{Boe}}{2}\frac{1}{\tan\theta_B} + \frac{1}{Z_0}) = j(-\frac{1}{Z_B\tan\theta_B} + \frac{1}{Z_0}) = 0$$

$$Y_{B12} = Y_{B21} = j\frac{Y_{Boo} - Y_{Boe}}{2}\cot\theta_B = j\frac{Y_B}{\tan\theta_B} = jY_0 \qquad (2.24)$$

where Y_0 is the characteristic admittance of the equivalent quarter-wave transmission line of the two kinds of coupled lines. Y_1 is assumed as the characteristic admittance from the input sight. Since it is a power splitter, the relationship below is satisfied

$$Y_0 = \frac{Y_1}{\sqrt{2}} \qquad (2.25)$$

Thus, the Y parameters of the whole tri-port circuit can be derived

$$[Y] = \begin{bmatrix} Y_{A11} + Y_{B11}\omega + j\omega C_A + j\omega C_B & Y_{A12} & Y_{B12} \\ Y_{A21} & Y_{A22} + j\omega C_A & 0 \\ Y_{B21} & 0 & Y_{B22} + j\omega C_B \end{bmatrix}$$

$$= \begin{bmatrix} 0 & -jY_0 & jY_0 \\ -jY_0 & 0 & 0 \\ jY_0 & 0 & 0 \end{bmatrix} = \begin{bmatrix} 0 & \dfrac{-jY_1}{\sqrt{2}} & \dfrac{jY_1}{\sqrt{2}} \\ \dfrac{-jY_1}{\sqrt{2}} & 0 & 0 \\ \dfrac{jY_1}{\sqrt{2}} & 0 & 0 \end{bmatrix} \qquad (2.26)$$

Based on the port terminations defined in Fig. 2.10, (2.26) can be converted to the scattering parameter matrix

$$[S] = ([Y_1] - [Y])([Y_1] + [Y])^{-1}$$

18

$$[S] = \begin{bmatrix} Y_1 - Y_{11} & -Y_{12} & -Y_{13} \\ -Y_{21} & Y_1 - Y_{22} & -Y_{23} \\ -Y_{31} & -Y_{32} & Y_1 - Y_{33} \end{bmatrix} \begin{bmatrix} Y_1 + Y_{11} & Y_{12} & Y_{13} \\ Y_{21} & Y_1 + Y_{22} & Y_{23} \\ Y_{31} & Y_{32} & Y_1 + Y_{33} \end{bmatrix}^{-1}$$

$$= \frac{1}{2Y_1^3} \begin{bmatrix} Y_1 & \dfrac{jY_1}{\sqrt{2}} & \dfrac{-jY_1}{\sqrt{2}} \\ \dfrac{jY_1}{\sqrt{2}} & Y_1 & 0 \\ \dfrac{-jY_1}{\sqrt{2}} & 0 & Y_1 \end{bmatrix} \begin{bmatrix} Y_1^2 & \dfrac{jY_1^2}{\sqrt{2}} & \dfrac{-jY_1^2}{\sqrt{2}} \\ \dfrac{jY_1^2}{\sqrt{2}} & \dfrac{3Y_1^2}{2} & \dfrac{Y_1^2}{2} \\ \dfrac{-jY_1^2}{\sqrt{2}} & \dfrac{Y_1^2}{2} & \dfrac{3Y_1^2}{2} \end{bmatrix} = \begin{bmatrix} 0 & \dfrac{j}{\sqrt{2}} & \dfrac{-j}{\sqrt{2}} \\ \dfrac{j}{\sqrt{2}} & \dfrac{1}{2} & \dfrac{1}{2} \\ \dfrac{-j}{\sqrt{2}} & \dfrac{1}{2} & \dfrac{1}{2} \end{bmatrix} \quad (2.27)$$

This is same with (2.16), the S matrix of the ordinary Marchand balun. It is the best attainable S parameter matrix of a lossless balun which is matched at the input ($S_{11}=0$) and has transmission coefficients of -3dB ($|S_{21}| = |S_{31}| = (1/2)^{1/2}$) with opposite phase. The outputs, however, are not matched or isolated. Both the output matching and isolation have a value of -6dB ($|S_{22}|= |S_{33}|=|S_{23}|= |S_{32}| =1/2$).

2.4 Isolation and Matching Network of Balanced Outputs

Most of the work on improving the planar balun can achieve a perfect matching at the unbalanced port, but its poor balanced port matching and isolation limits its applications. For example, an extra output impedance-transforming matching network is needed for a push-pull amplifier design if a balun is applied at the power amplifiers' output.

To achieve perfect output port matching and isolation, some form of resistive network need to be added between the output ports which are drawn in Fig.2.11, just as in the Wilkinson power divider. Y parameters will be used to derive the required resistive network. The S parameters matrix of a balun with perfect output

19

matching and isolation has the form [22]

$$[S]perfect = \begin{bmatrix} 0 & \dfrac{j}{\sqrt{2}} & \dfrac{-j}{\sqrt{2}} \\ \dfrac{j}{\sqrt{2}} & 0 & 0 \\ \dfrac{-j}{\sqrt{2}} & 0 & 0 \end{bmatrix} \qquad (2.28)$$

Similarly, the S matrix in (2.28) is converted to the Y matrix

$$[Y]perfect = \begin{bmatrix} 0 & \dfrac{-jY_1}{\sqrt{2}} & \dfrac{jY_1}{\sqrt{2}} \\ \dfrac{-jY_1}{\sqrt{2}} & \dfrac{Y_1}{2} & \dfrac{Y_1}{2} \\ \dfrac{jY_1}{\sqrt{2}} & \dfrac{Y_1}{2} & \dfrac{Y_1}{2} \end{bmatrix} \qquad (2.29)$$

Comparing (2.26) and (2.29), it can be deduced that the Y matrix of the resistive network has the form

$$[Y]_R = \frac{1}{2Z_1} \begin{bmatrix} 1 & 1 \\ 1 & 1 \end{bmatrix} \qquad (2.30)$$
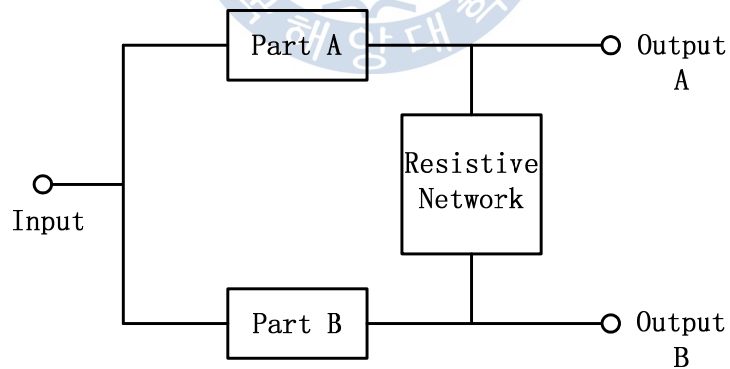

Fig. 2.11 Sketch of perfect output port matching and isolation balun with resistive network

The resistive network can be realized by a series connection of a phase inverter and a resistor of value $2Z_1$, Nevertheless, the phase inverter proposed in [22] is realized by a simple half-wavelength transmission line. This bulky resistive network consumes a large circuit area. In [33], a new technique using a physically short phase inverter network in proposed. A coupled line section grounded at each end acts as a phase inverter which takes the place the half-wavelength transmission line. Albeit it can save the circuit proportion partly, as the electrical length of the coupled lines is reduced, Z_{oo} becomes too small to achieve in a physical structure by the technique until now. For example, if the electrical length of the couple line is chosen as 15 degree, the odd mode characteristic impedance Z_{oo} is just 3 Ohm. It means the slot of the coupled lines is unimaginable small if realize it on PCB.

Whereas, the resistive network could achieve the miniaturization easily through replacing the half-wavelength transmission line in [22] by diagonally shorted coupled lines with shunted lumped capacitors mentioned above as the phase inverter. Fig. 2.12 shows the schematic diagram of the perfectly matched balun with the improved resistive network. By choosing the same electrical length of 15 degree, the improved method in our thesis is more feasible because of the adjustable capacitors.
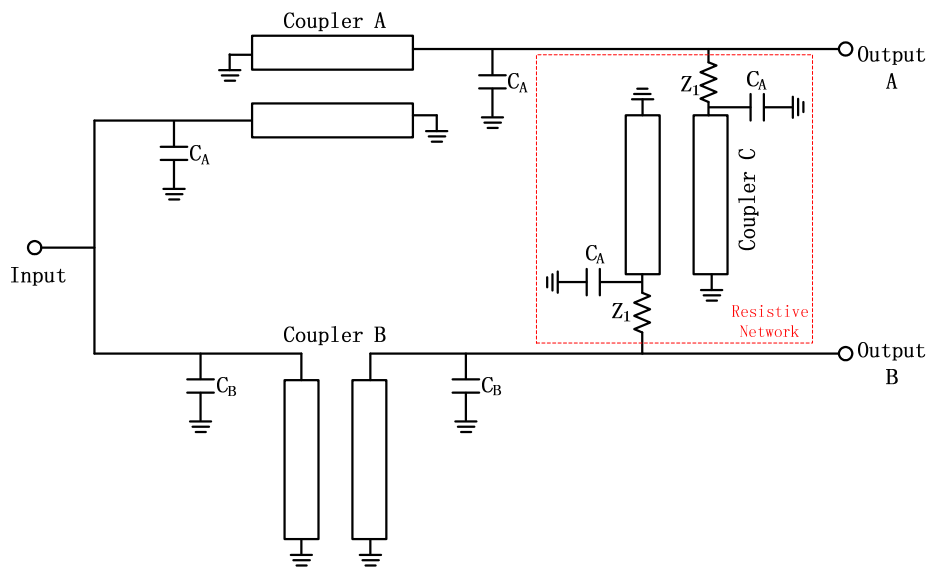
Fig. 2.12 Schematic diagram of the perfectly matched balun with improved resistive network

CHAPTER 3 Simulation, Fabrication and Measurement

From the above analysis, the coupled lines with high characteristic impedance and short electronic length are required for the miniaturized balun filter. To validate the analytical results and demonstrate the design approach, the circuit parameters are converted to physical filter structures and simulated by circuit simulation software Agilent Advanced Design System (ADS) and full-wave 3-D EM simulation tool Ansoft HFSS. For the sake of simplifying the fabrication procedure as easy as can be realized in author's laboratory room, the circuit is implemented on printed circuit board (PCB). The ideal specifications of the proposed balun filter are listed in Table 3.1.

Table 3.1 Ideal specifications of the proposed balun filter

Center frequency (GHz)	1 GHz
Fractional bandwidth (%)	20%
Insertion loss (dB)	-3 dB
Stopband rejection (dB)	< -60 dB up to 10 f_0

3.1 Circuit Simulating by ADS and Analysis

Although the ADS simulation and calculation are carried out in ideal cases, which have not taken many potential factors that may affect the performances of the balun into consideration. As its simulation speed is much faster than HFSS and the alteration tendency of the result can be observed easily while the circuit factors are tuning. Generally, simulation is carried out by ADS at the first step.
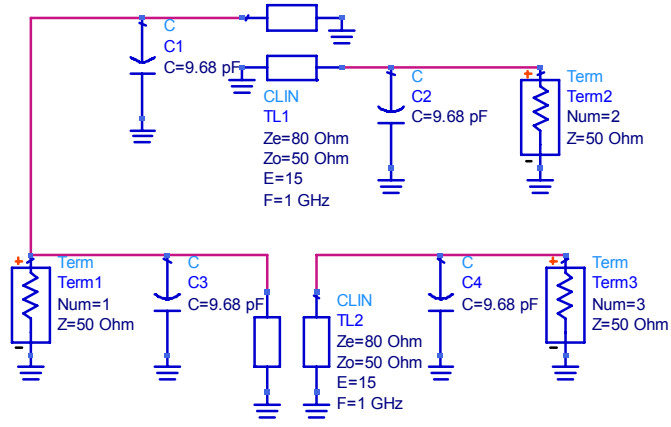
The initial miniaturized balun filter model illustrated in Fig. 2.10 with electrical length of coupled-line being 15° was obtained. When the even-mode impedance Z_{oe} was arbitrarily chosen as 80Ω, the value of the lumped capacitor C_A and C_B was calculated to be 9.68 pF according to the equations (2.5) and (2.10) and the odd-mode impedance of the coupled-line Z_{oo} was 50Ω, making the coupling coefficient K being 0.23. The coupling coefficient K of the shorted coupled-line can determine the bandwidth of the proposed balun filter. The bandwidth increases as the coupling coefficient K does [34].

$$K = \frac{Z_{oe} - Z_{oo}}{Z_{oe} + Z_{oo}} \qquad (3.1)$$

When the quarter-wavelength transmission line was miniaturized, one can choose a proper coupling coefficient according to the required bandwidth of the bandpass filter. However, to achieve a broad bandwidth, the coupling coefficient K should be made as large as possible, which means the difference between Z_{oe} and Z_{oo} should be large. It will result in a small characteristic impedance of the coupled lines and hence a large electrical length of them. Therefore, a necessary design trade-off between broad bandwidth and small circuit size should be considered.

With the obtained circuit parameters, the ADS model of the initial size-reduced balun filter was built as given in Fig. 3.1 (a) and its frequency and phase response are also shown in Fig. 3.1 (b), (c) and (d), respectively, from which we can observe the great agreement with our expectation.
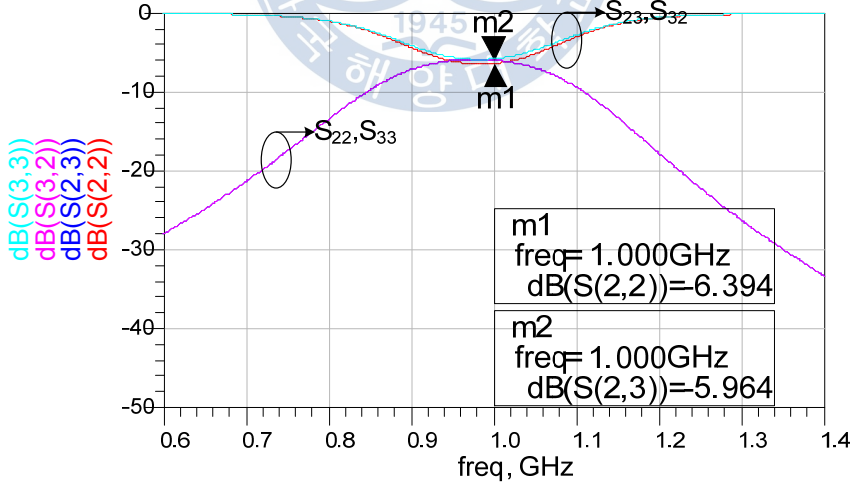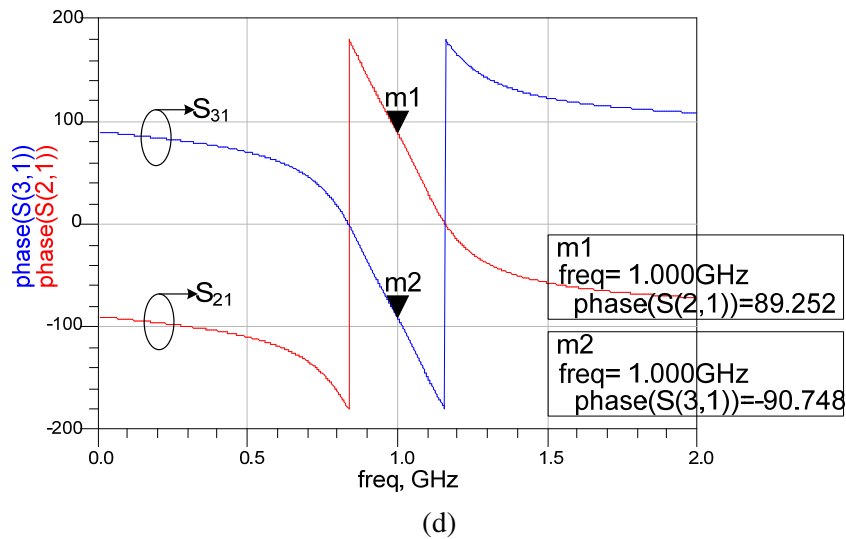
24

(a)

(b)

(c)

25

(d)
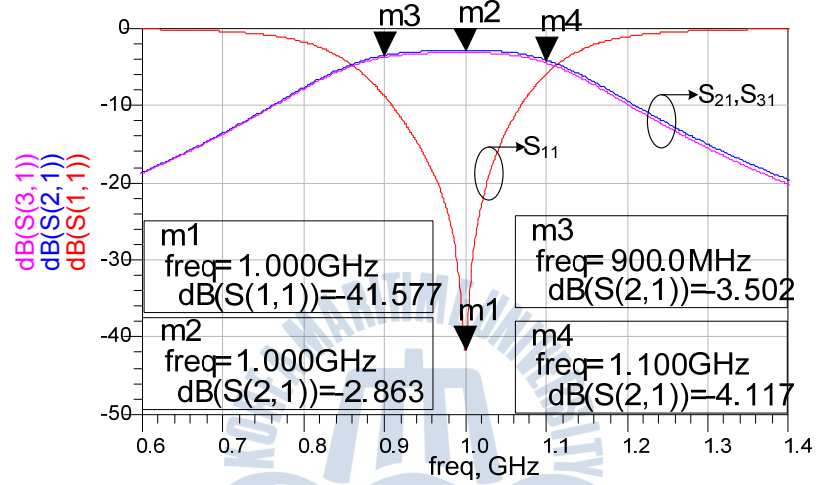
Fig. 3.1 ADS model of the initial miniaturized balun filter (a) and its frequency response of S_{11}, S_{21} and S_{31} (b), S_{22}, S_{23}, S_{32} and S_{33} (c) and phase response (d)

In many filter application, in order to reduce interference by keeping out-of-band signals from reaching a sensitive receiver, a wider upper stopband is required. However, many planar filters which are comprised of half-wavelength resonators have an inherently spurious passband at $2f_0$, where f_0 is the center frequency. In this thesis, the proposed filter is reduced to just 15 degree using combinations of two kinds of parallel coupled lines and shunt lumped capacitors. Therefore, the first spurious frequency can be shifted to much higher frequency for the electrical length of the resonant is very small.

The broadband transmission characteristic of the ADS simulation result is illustrated in Fig. 3.2. It could be noted that there is no spurious response occurs for the frequency below 10GHz. In this case, the first spurious frequency is shifted to the position which is more than 10 times of the fundamental frequency.
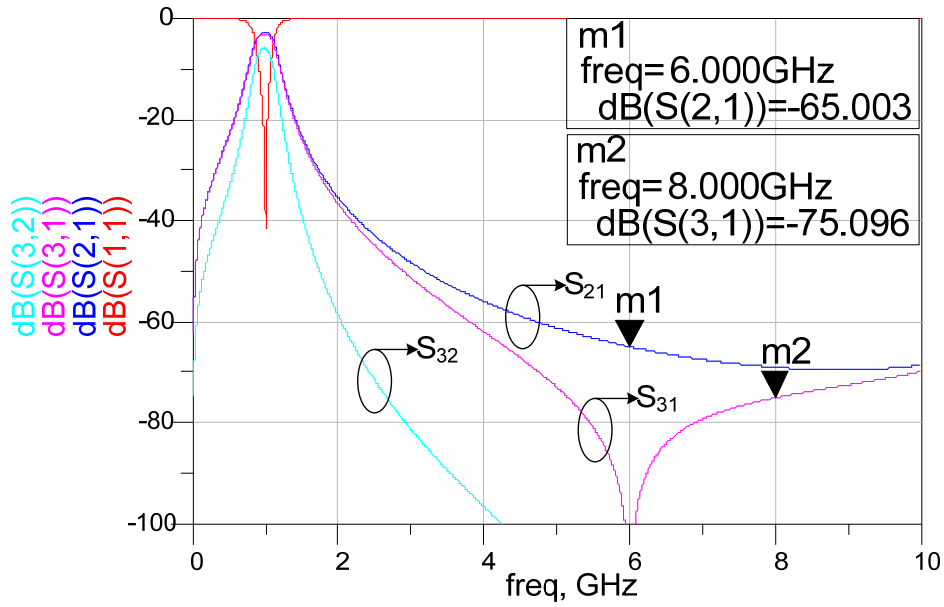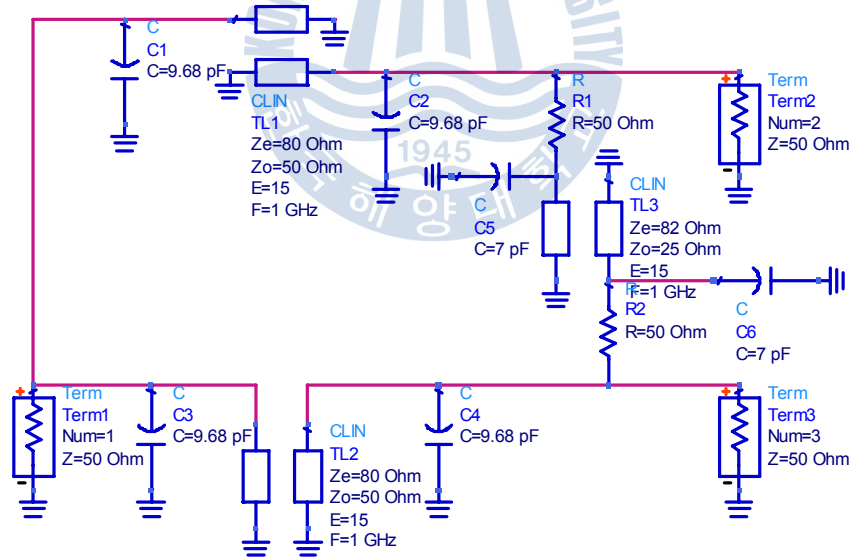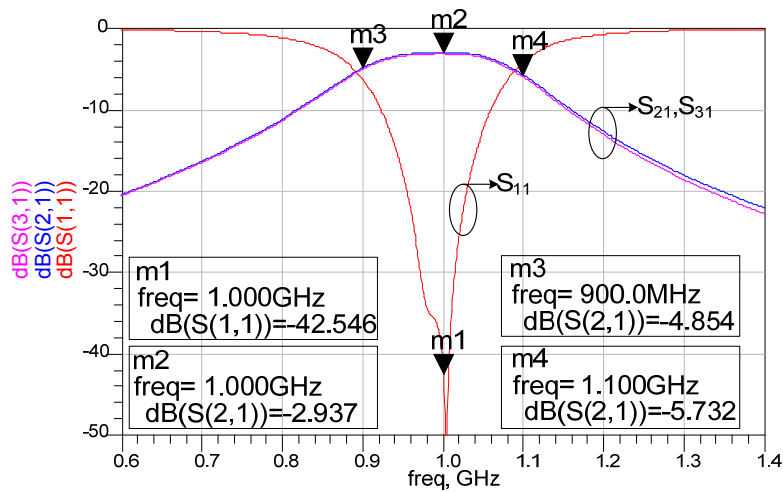
26

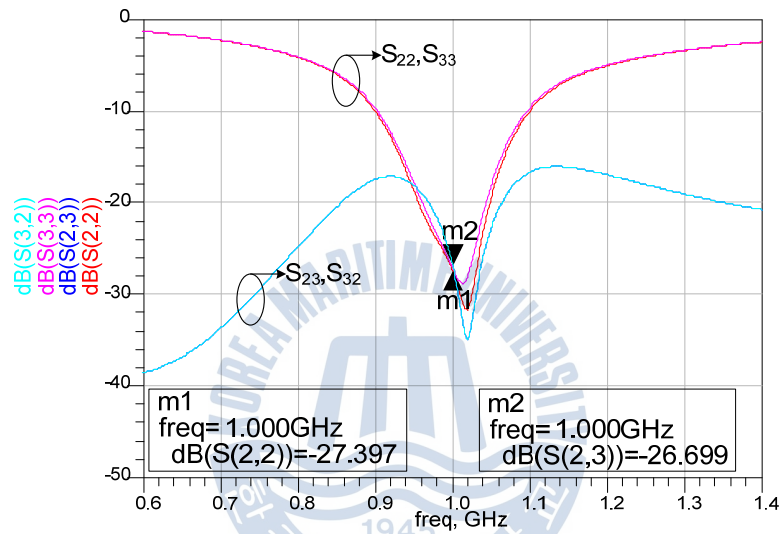*Fig. 3.2 ADS simulation result in broad frequency range*

Fig. 3.3 shows the simulation model (a) and results (b) and (c) of the perfectly

matched balun with the improved resistive network.

(a)

27

(b)

(c)

Fig. 3.3 ADS model of the perfectly matched balun with improved resistive network (a) and its frequency response of S_{11}, S_{21} and S_{31} (b), S_{22}, S_{23}, S_{32} and S_{33} (c)

3.2 Full-Wave EM Simulation by HFSS and Optimization

The theoretical values calculated through the deduced equations have been confirmed through ADS simulation. And the width and length of each coupled line can be obtained by ADS Line Calculation Tool, as given in Fig. 3.4.
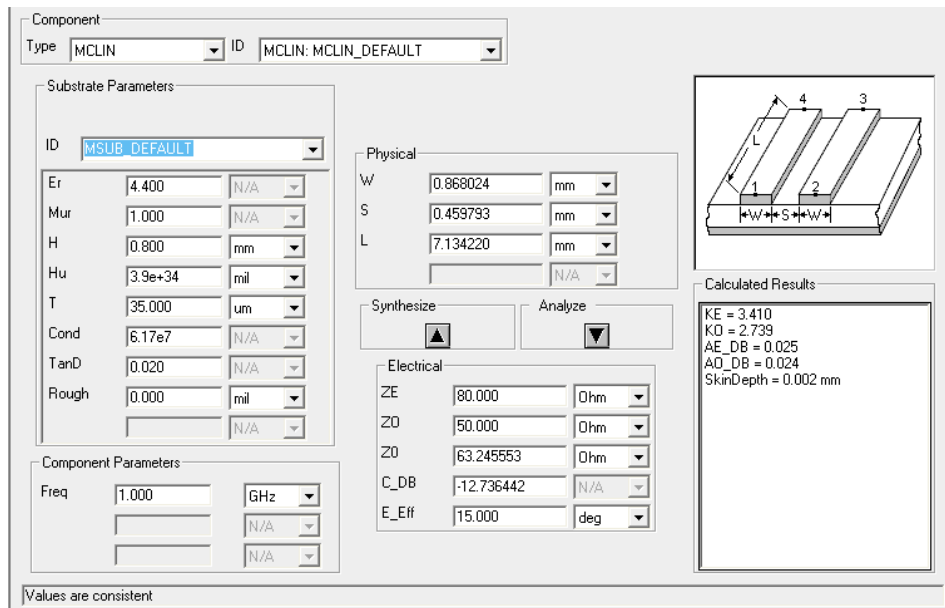
*Fig. 3.4 Detailed value of coupled lines calculated by ADS Linecalc*

Once the bandpass filter equivalent circuit model was developed, physical filter structures such as resonators and coupled-line sections can be designed. However, one thing needs to be kept in mind: the synthesized filter model cannot be transformed into physical structures at one shot due to the parasitic components (both internally and externally). As a result, either an optimization of the filter physical dimensions or a tuning of the filter responses is necessary. Usually, it is carried out with Ansoft HFSS before fabrication until the EM simulation shows a performance close to the target one.

Table 3.2 gives the design parameters of the HFSS simulation. Fig. 3.5 (a), (b) and (c) show the layout of the balun filter drawing in HFSS and its two kinds of simulation results, respectively. Since considering the reciprocity between physical lines and optimizing the results to an expecting one. The values of the coupled lines

element have been modified slightly. We can observe that the balun filter responses simulated by the full-wave simulator are almost the same as the responses optimized by the circuit simulator ADS. This proves the validity of this design method.

Table 3.2 Design parameters of the HFSS simulation

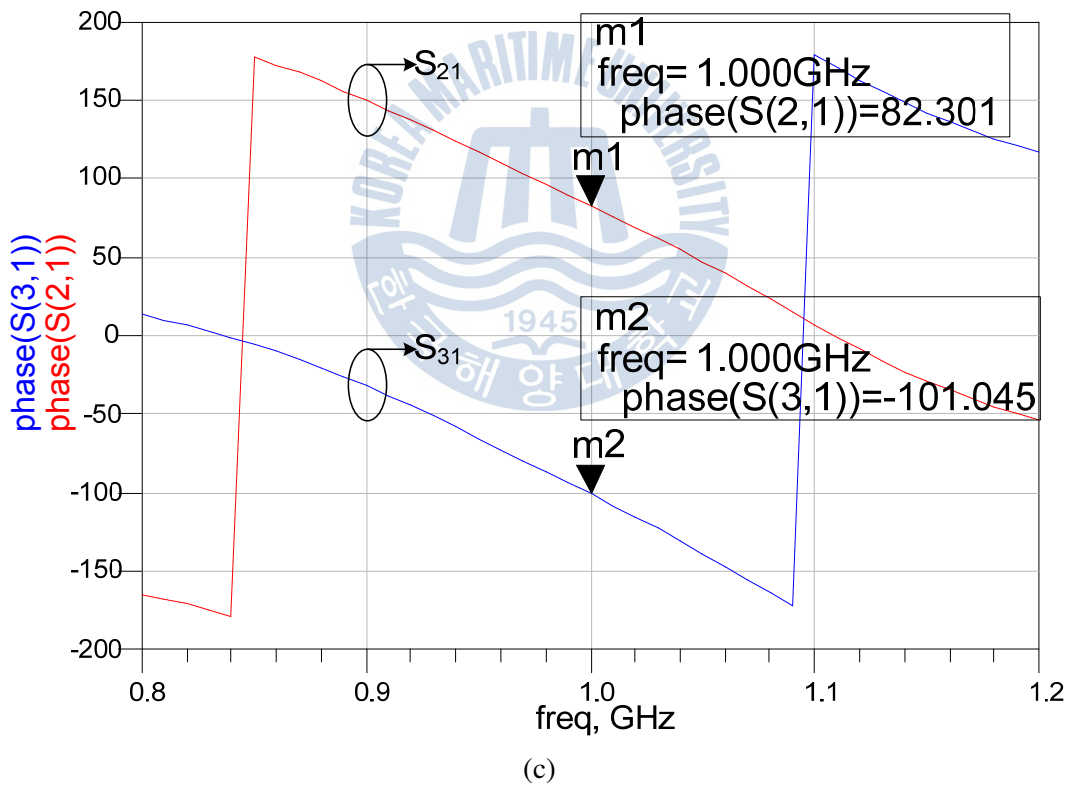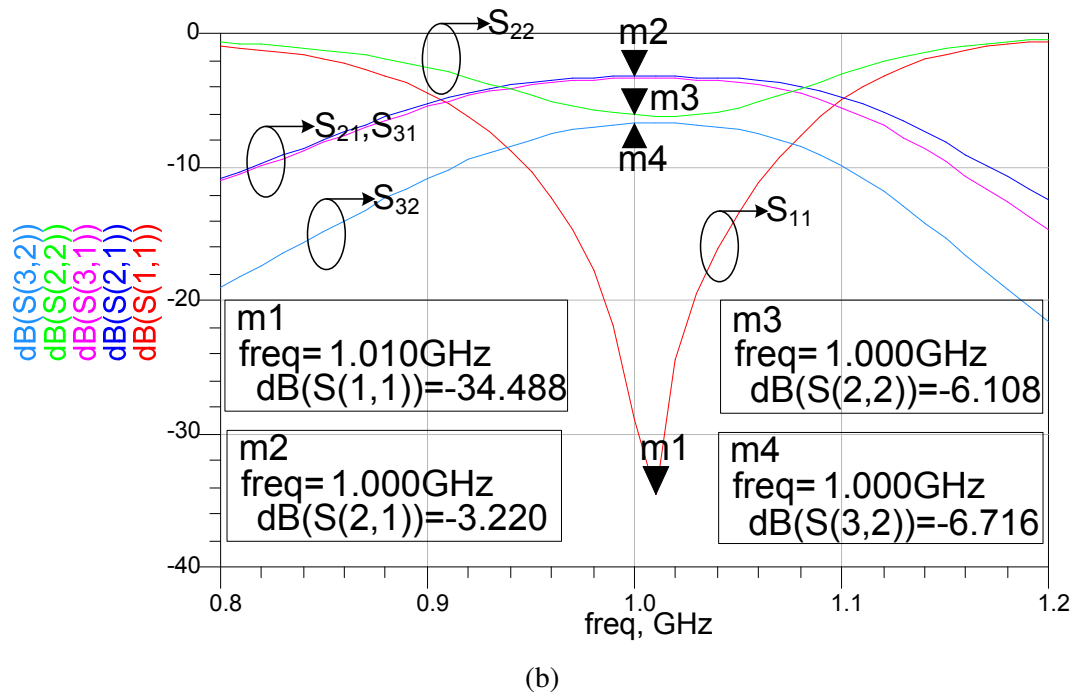| Center frequency	1GHz
Substrate thickness	0.8 mm
Substrate permittivity	4.4
Dielectric loss tangent	0.02
Copper thickness	35μm
Copper conductivity	6.17×10^7
Width of coupled lines	0.65 mm
Length of coupled lines	8.2 mm
Slot of coupled lines	0.54 mm
Capacitor	5.5 pF
Width of transmission line	1.2 mm
Ports impedance	50 Ohm
Circuit size	30 mm×10 mm

(a)

30
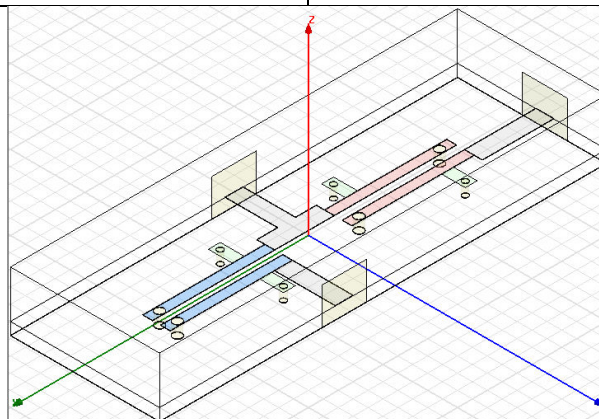
Fig. 3.5 Layout of balun filter drawn by HFSS (a), its frequency response (b) and phase response (c)

31

3.3 Fabrication and Measurement

The layout of the balun filter used in fabrication which is drawn through Auto Computer Aided Design (AutoCAD) is given in Fig. 3.6 (a), with the dimensions of the circuit area being 10mm×30mm. The balun filter is realized on the FR4 epoxy glass cloth copper-clad plat (CCL) PCB substrate having thickness 0.8mm and dielectric constant ε_r=4.4. For the measurement convenience, all the balanced and unbalanced ports impedances are assumed to be 50Ohm. The photograph of the fabricated balun is displayed in Fig. 3.6 (b).

The measured performances of the fabricated 1GHz balun filter and the comparison with HFSS simulation results are plotted in Fig. 3.7 and Fig. 3.8. The insertion loss of simulation result by HFSS is -3.22dB and measurement result is -4.2dB. It shows equal power splitting performance and good phase response. Additional loss is caused by surface and edge roughness of the metal, inferior metal conductivity, the dielectric loss of the substrate and the inexactness of fabrication technology and so on, which were not taken into account in the calculations.

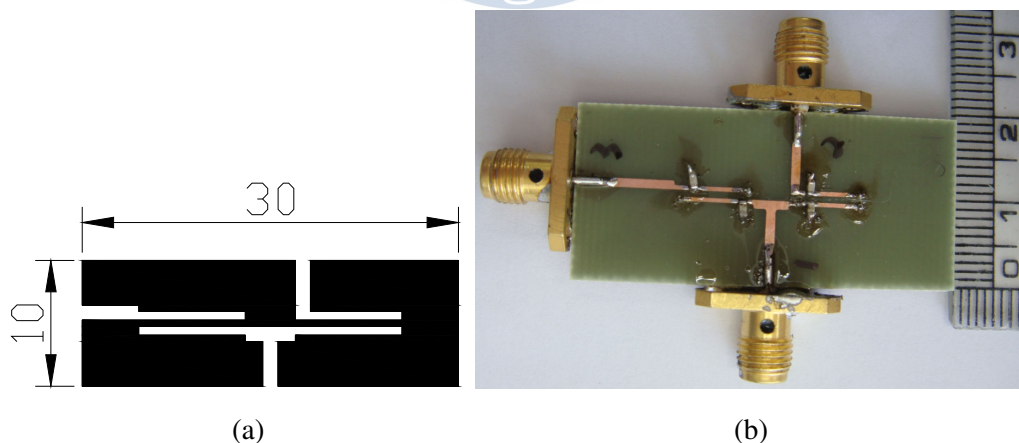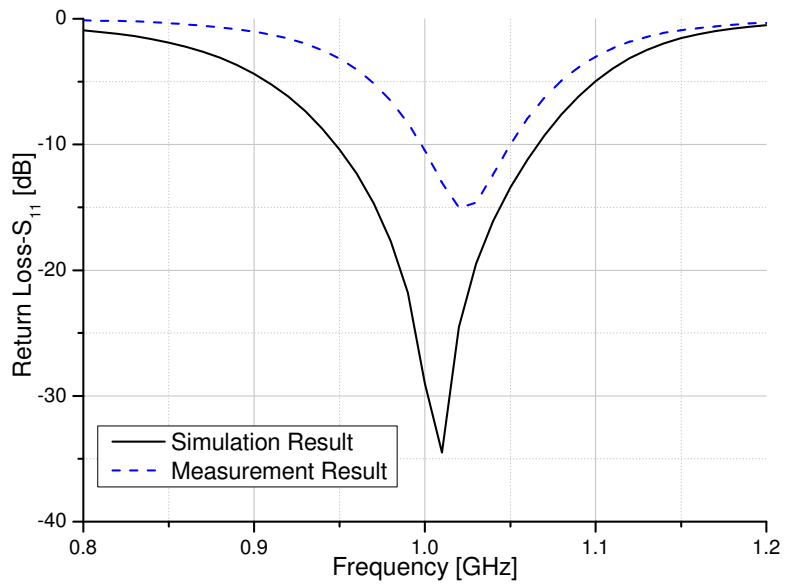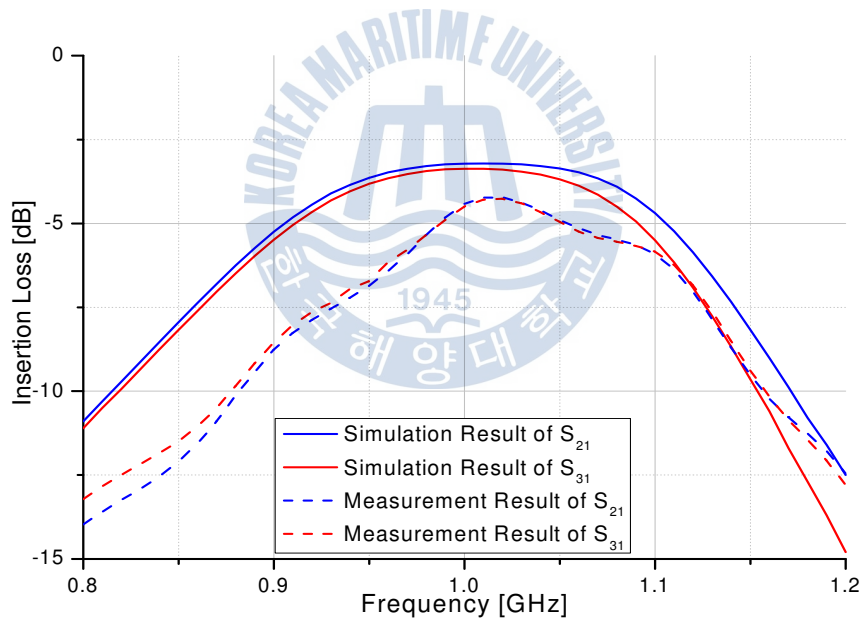(a)   (b)

Fig. 3.6 Layout of fabrication circuit drawn through AutoCAD (a) and its photograph (b)

32

(a)

(b)

33

(c)
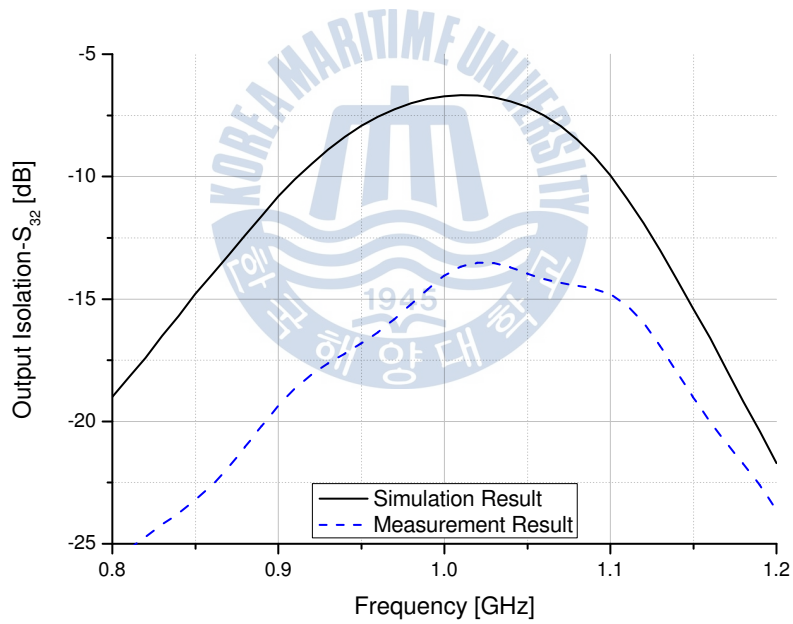
(d)

Fig. 3.7 Measured frequency performances compared with HFSS simulation results of input return loss S_{11} (a), insertion loss S_{21} and S_{31} (b), outputs return loss S_{22} and S_{33} (c) and outputs isolation S_{32} (d)
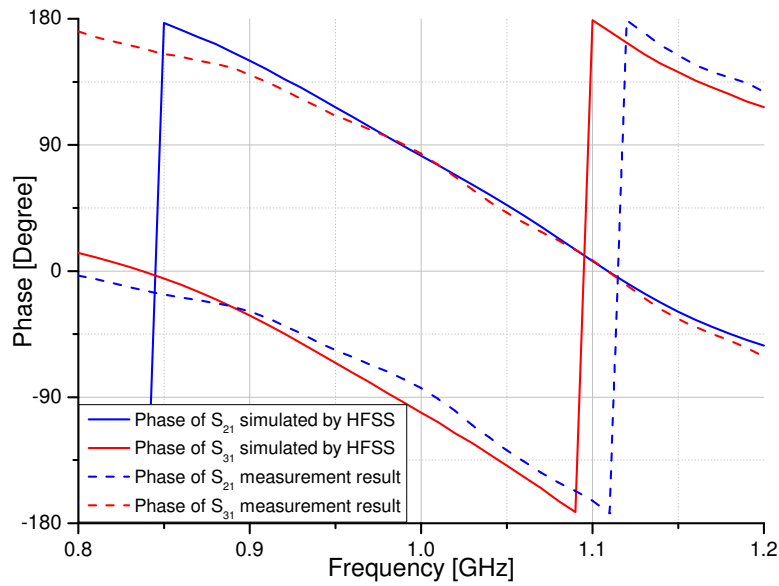
Fig. 3.8 Measured phase response compared with HFSS simulation result

The perfectly matched balun filter with improved center resistive network is also fabricated and measured by inserting the coupled line with length of 7.44mm, width of 1.01mm, slot of 0.03mm and capacitor value of 3pF. Its photograph is displayed in Fig. 3.9. The total size of the circuit is 26mm×30mm, not including the extended space for testing. Fig. 3.10 shows the measured results.

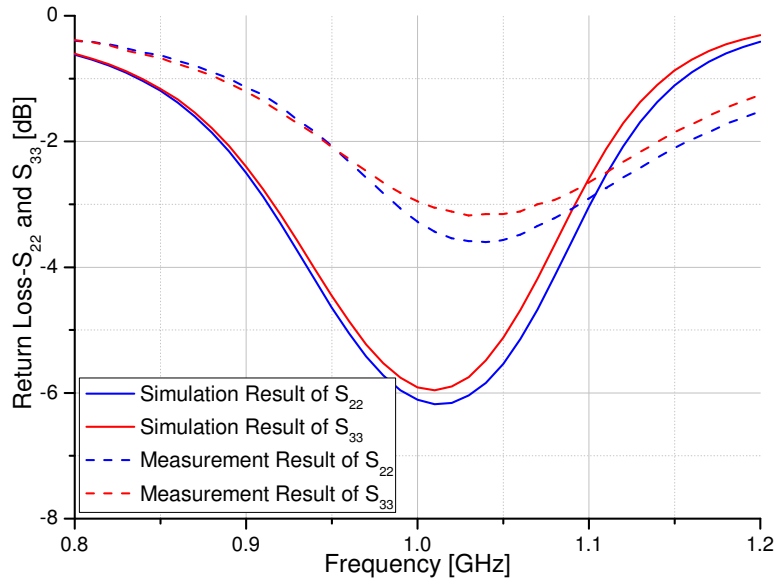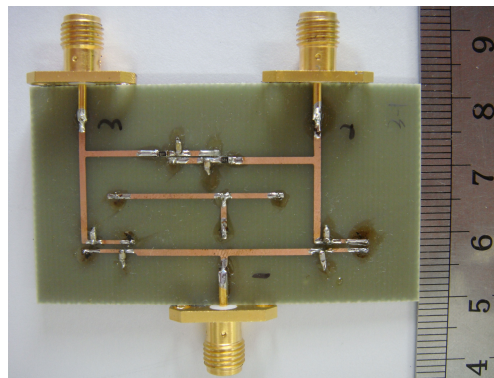*Fig. 3.9 Photograph of perfectly matched balun filter with improved resistive network*

35

(a)

(b)

36
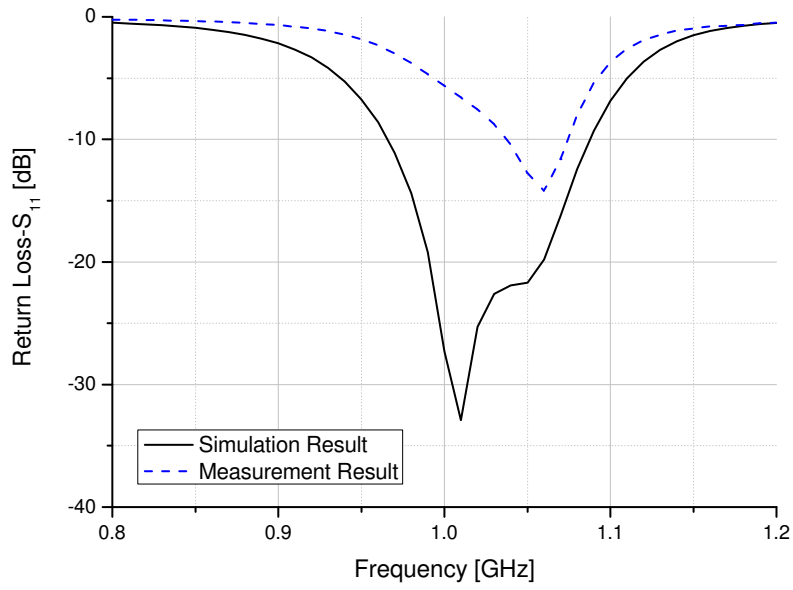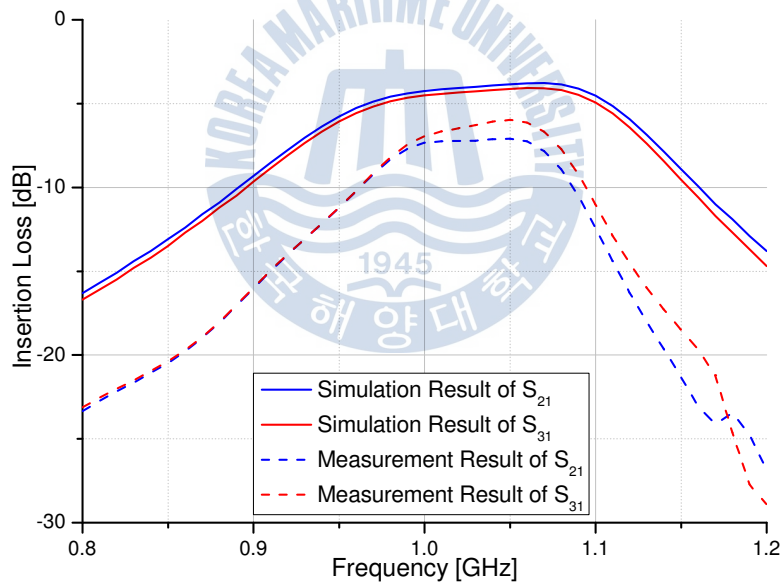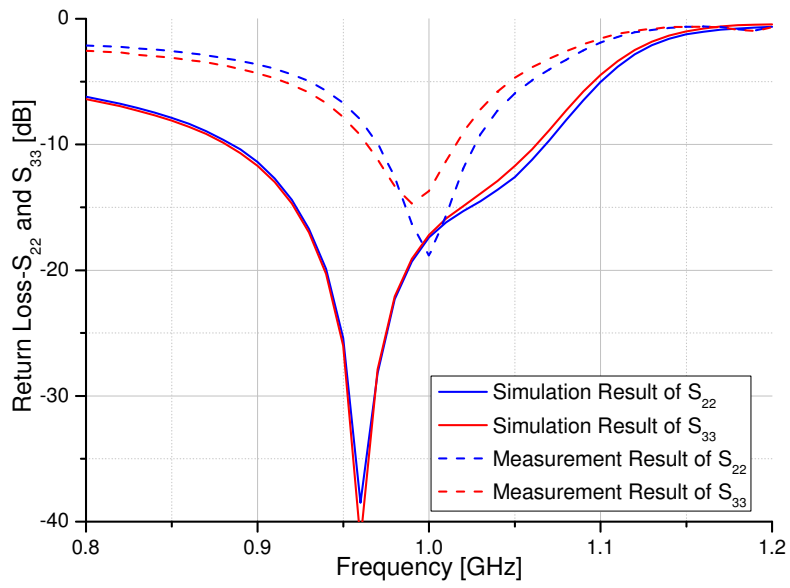
(c)
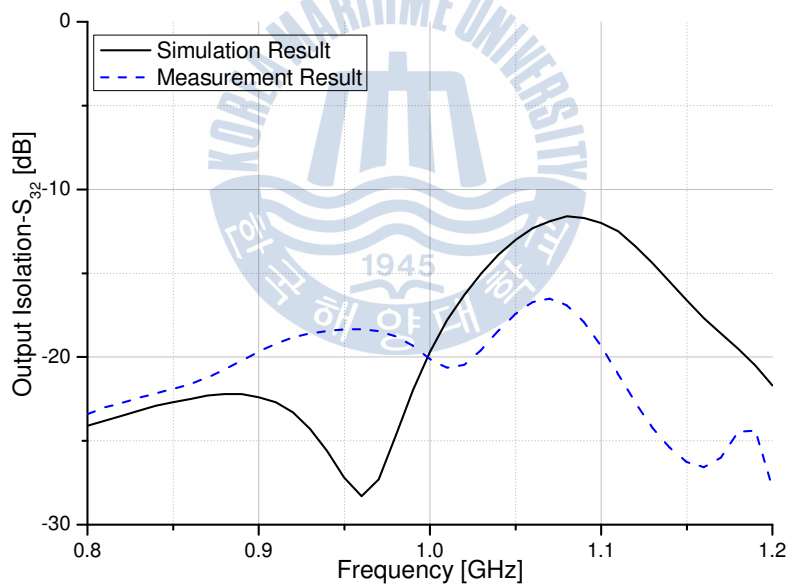
(d)

Fig. 3.10 Measured performances compared with HFSS simulation results of perfectly matched balun filter with resistive network

Finally, Table 3.3 summarizes the characteristic of several published bandpass balun filters in comparison with this work. Obviously, the proposed bandpass filter in this paper shows the advantage of more compact size, excellent insertion loss characteristic, and broad bandwidth performance.

Table 3.3 Comparison of different types of balun filter

Reference	Technology	Center Frequency (GHz)	FBW	Insertion Loss (dB)	Die Area (mm^2)	Year
[35]	PCB	2	$0.05f_0$	-3.9	20×20	2009
[36]	PCB	2.7	$0.11 f_0$	-4.43	14.9×15.2	2010
[37]	PCB	2.45	$0.041f_0$	-4.34	50×41	2011
[38]	PCB	3.48	$0.017f_0$	-4.9	7×7	2011
[39]	PCB	3	$0.087f_0$	-5.33	50×50	2011
[40]	PCB	1	$1.12f_0$	-4.07	33×80	2012
This work	PCB	1	$0.23f_0$	-4.2	10×30	2012
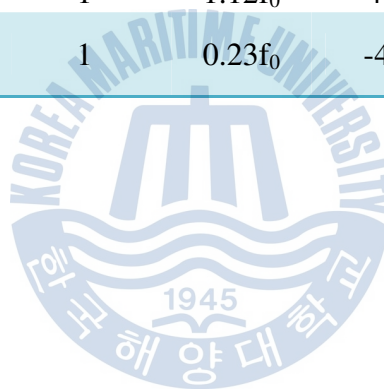
Chapter 4 Conclusion

In this thesis, the design theory and procedure for a novel enhanced balun bandpass filter for extremely miniaturization is carried out utilizing the combination of diagonally shorted coupled lines and parallel end shorted coupled lines both with shunt lumped capacitors which offers great amplitude and phase balance performance. A technique for achieving output matching and isolation has also been proposed. The method of adding shunt lumped capacitors to the conventional coupled line section can largely reduce the required electrical length. It shows a wider upper stopband and broad bandwidth over the operating frequency.

To demonstrate the feasibility and validity of the design equation, the size of 10mm×30mm, not including the extended space for testing, miniaturized balun filter is designed and fabricated on PCB substrate with the thickness of 0.8mm. The electrical length of the coupled lines is reduced to 15 degree. According to the measurement results, it exhibits a bandwidth of 100MHz and 180 degree phase difference at a center frequency of 1GHz. The measurement responses agree well with simulation result curves. This class of perfectly matched baluns is invaluable in the design of balanced microwave circuits.

References

[1]   T. Chen *et al.*, "Broadband monolithic passive baluns and monolithic double balanced mixer", *IEEE Trans. Microwave Theory Tech.*, vol. 39, pp. 1980–1986, Dec. 1991.

[2]   S. C. Tseng, C. C. Meng, C. H. Chang, C. K. Wu and G. W. Huang, "Monolithic broadband Gilbert micromixer with an integrated Marchand balun using standard silicon IC process", *IEEE Trans. Microwave Theory Tech.*, vol. 54, no. 12, pp. 4362–4371, Dec. 2006.

[3]   P. C. Hsu, C. Nguyen and M. Kintis, "Uniplanar broad-band push–pull FET amplifiers", *IEEE Trans. Microwave Theory Tech.*, vol. 45, pp. 2150–2152, Dec. 1997.

[4]   S. A. Maas and Y. Ryu, "A broadband, planar, monolithic resistive frequency doubler", *IEEE Int. Microwave Symp. Dig.*, pp. 443–446, 1994.

[5]   A. M. Pavio and A. Kikel, "A monolithic or hybrid broadband compensated balun", *IEEE MTT-S Int. Dig.*, pp. 483–486 , 1990.

[6]   K. C. Gupta and C. Cho, "A new design procedure for single-layer and two-layer three-line baluns", *IEEE Trans. Microwave Theory Tech.*, vol. 46, no. 12, pp. 2514–2519, Dec. 1998.

[7]   W. K. Roberts, "A new wide-band balun", *Proc. IRE,* vol. 4.5, pp. 1628–1631, Dec.1957.

[8]   M. Rajashekharaiah, P. Upadhyaya and H. Deukhyoun, "A compact 5.6 GHz low noise amplifier with new on-chip gain controllable active balun", in *Proc. IEEE Workshop Microelectron Electron Devices*, pp. 131–132, 2004.

[9]   Y. J. Yoon, Y. Lu, R. C. Frye, M. Y. Lau, P. R. Smith, L. Ahlquist and D. P. Kossives, "Design and characterization of multiplayer spiral transmission- line baluns", *IEEE Trans. Microwave Theory Tech.*, vol. 47, no. 9, pp. 1841–1847, Sep. 1999.

[10] B. A. Munk, *Balun, etc.*, 3rd ed, J. D. Kraus and R. J. Marhefka, Eds. New York: McGraw-Hill, ch. 23, 2002.

[11] N. Marchand, "Transmission-Line Conversion Transformers", *Electronics*, vol. 17, pp. 142–146, Dec. 1944.

[12] W. R. Brinlee, A. M. Pavio and K. R. Varian, "A novel planar double -balanced 6–18 GHz MMIC mixer", *IEEE Microwave Millimeter-Wave Monolithic Circuit Symp. Dig.*, pp. 139–142, 1994.

[13] M. C. Tsai, "A new compact wide-band balun", *IEEE Microwave and Millimeter Wave Monolithic Circuit Symp. Dig.*, pp. 123–125, 1993.

[14] K. Nishikawa, I. Toyoda and T. Tokumitsu, "Compact and broad-band

three-dimensional MMIC balun". *IEEE Trans. Microwave Theory Tech.*, vol. 47, pp. 96–98, Jan. 1999.

[15] N. E. Lindenblad, "Television transmitting antenna for Empire State Building ", *RCA Rev.*, vol. 3, pp. 387-408, Apr. 1939.

[16] Radio Research Laboratory Staff, *Very High-Frequency Techniques.* New York: McGraw-Hill, vol. 1, p. 88, 1947.

[17] H. G. Oltman, Jr., "Analysis of the compensated balun", *Rantec Corp., Calif., Tech. Rept.,* May 1961.

[18] J. W. McLaughlin, D. A. Dunn, and R. W. Grow, "A wide-band balun", *IRE Trans. on Microwave Theory and Techniques,* vol. MTT- 6, pp. 314-316, July 1958.

[19] R. Bawer and J. J. Wolfe, "A printed circuit balun for use with a spiral antenna", *IRE Trans. on Microwave Theory and Techniques,* vol. MTT-8, pp. 319–325, May 1960.

[20] R. Schwindt and C. Nguyen, "Computer-aided analysis and design of a planar multilayer Marchand balun", *IEEE Trans. Microwave Theory Tech.*, vol. 42, pp. 1429–1434, July 1994.

[21] C. S. Lin, P. S. Wu, M. C. Yeh, J. S. Fu, H. Y. Chang, K. Y. Lin, and H. Wang, "Analysis of multiconductor coupled-line Marchand baluns for miniature MMIC design", *IEEE Trans. Microw. Theory Tech.*, vol. 55, no. 6, pp. 1190–1199, Jun. 2007.

[22] K. S. Ang and I. D. Robertson, "Analysis and design of impedance transforming Marchand balun", *IEEE Trans. Microwave Theory Tech.*, vol. 49, pp. 402–405, Feb. 2001.

[23] S. B. Cohn, "Parallel-coupled transmission-line-resonator filters", *IRE Trans. Microw. Theory Tech.*, vol. MTT-6, no. 4, pp. 223–231, Apr. 1958.

[24] G. L. Matthaei, "Design of wide-band (and narrow-band) bandpass microwave filters on the insertion loss basis", *IRE Trans. Microw. Theory Tech.*, vol. MTT-8, no. 11, pp. 580–593, Nov. 1960.

[25] C. Y. Chang and T. Itoh, "A modified parallel-coupled filter structure that improves the upper stopband rejection and response symmetry", *IEEE Trans. Microw. Theory Tech.*, vol. 39, no. 2, pp. 310–314, Feb. 1991.

[26] A. Riddle, "High performance parallel coupled microstrip filters", in *IEEE MTT-S Int. Microwave Symp. Dig.*, pp. 427–430, 1988.

[27] D. M. Pozar, *Microwave Engineering*, 2nd ed. New York: Wiley, pp. 474–485, 1998.

[28] T. Hirota, "Reduced-size branch-line and rat-race hybrids for uniplanar MMIC's", *IEEE Trans. Microwave Theory Tech.,* Vol.38, No. 3, March 1990

[29] G. Matthaei, L. Young, E. M. T. Jones, *Microwave Filters, Impedance*

-*Matching networks, and Coupling Structures,* Artech House, pp.220.

[30] I. Kang and J. Choi, "A new reduced-size lumped distributed power divider using the shorted coupled line pair", *Korea Electromagnetic Engineering Conference,* vol.13, No.1, pp283-287, Nov. 2003.

[31] I. Kang and J. S. Park, "A reduced-size power divider using the coupled line equivalent to a lumped inductor", *Microwave Journal*, vol. 46, no. 7, Jul. 2003.

[32] G. I. Zysman and A.K. Johnson, "Coupled transmission line networks in an inhomogeneous dielectric medium", *IEEE Trans. Microwave Theory Tech.,* vol. MTT-17, No. 10, pp.753-759, Oct. 1969.

[33] M. Chongcheawchamnan, C. Y. Ng, K. Bandudej, A. Worapishet and I. D. Robertson, "On Miniaturization Isolation Network of an All-Ports Matched Impedance-Transforming Marchand Balun", *IEEE Microwave and Wireless Components Letters,* Vol. 13, No. 7, pp. 281-283, Jul. 2003.

[34] I. Kang and K. Wang, "A broadband rat-race ring coupler with tightly coupled lines", *IEICE Trans. Commun.*, vol. E88-B, no. 10, pp. 4087-4089, Oct. 2005.

[35] T. Yang, M. Hashemi, T. Itoh, "Compact Balun Filter Based On Negative and Zeroth Order Resonances Using Mushroom Structures", *Proceedings of the 39th European Microwave Conference*, pp. 354-357, Sept. 2009.

[36] T. Yang, M. Tamura, T. Itoh, "Compact hybrid resonator with series and shunt resonances used in miniaturized filters and balun filters", *IEEE Trans. Microw. Theory Tech*, 58, (2), pp. 390–402, 2010.

[37] S. J. Kang, H. Y. Hwang, "Ring-balun-bandpass filter with harmonic suppression", *IET Microw. Antennas Propag*, Vol. 4, Iss. 11, pp. 1847–1854, 2010.

[38] S. Sun and W. Menzel, "Novel Dual-Mode Balun Bandpass Filters Using Single Cross-Slotted Patch Resonator", *IEEE Microwave and Wireless Components Letters,* Vol. 21, No. 8, pp.415-417, Aug 2011.

[39] C. H. Ng, E. H. Lim, K. W. Leung, "Compact Microstrip Patch Balun Filter", *2011 Cross Strait Quad-Regional Radio Science and Wireless Technology Conference,* pp.1749-1751, 2011.

[40] Y. Lin, J. Lu, C. Chang, "Design of High-Order Wideband Planar Balun Filter in S-Plane Bandpass Prototype", IEEE Transactions on Microwave Theory and Techniques, vol. 99, pp. 1-7, 2012.

Acknowledgement

I would like to acknowledge a number of people who have helped me during the past two years. There is no way for me to finish this thesis without their supports and encouragements.

First and foremost, my greatest appreciation surely belongs to Prof. In-Ho Kang, who guided me through the M.S. program. His creativity, broad knowledge and insight into the circuit design helped me avoid going down wrong path and shortened the path to achieve the project goal. His energy and love of what he is doing inspires me a lot. I feel very grateful for his supervision both on the technical and the personal levels during my stay in Korea.

I would also like to express my sincere gratitude to the other professors of our school for their guidance. I am particularly grateful to my thesis committee members Prof. Young Yun and Prof. Dong-Kook Park for their time and valuable suggestions in guiding and reviewing my work. My acknowledgement will not be complete without mentioning the staff members of the Department of Radio Science and Engineering for their dedication and assistance.

I want to thank all the past and present members of the RF Circuit & System Lab, especially Mr. Kai Wang and Mr. Xu-Guang Wang, for their professional and personal supports. There is also my gratitude to all other friends at Korea Maritime University for the friendly environment and emotional supports. I will not forget the time we spent together before and in the future.

Additionally, I am deeply indebted to Prof. Ying-Ji Piao at Qingdao University. Without her recommendation, it is impossible for me to get this great opportunity to study in Korea.

Finally, I would like to dedicate this thesis to my family for their continued love and strong supports throughout all these years. You are always the persons who believe in and encourage me in all my endeavors, which is a contributing factor to any success I may achieve. Without these endless and priceless loves, it will never be possible for me to still live happily and accomplish my tasks. I feel great fortune to have you all accompany with me, only in this way, my life is complete and honorable.